THE JOURNAL OF PHYSICAL CHEMISTRY A

ARTICLE

pubs.acs.org/JPCA

Membrane Position of Ibuprofen Agrees with Suggested Access Path Entrance to Cytochrome P450 2C9 Active Site

Karel Berka,[†] Tereza Hendrychová,[†] Pavel Anzenbacher,[‡] and Michal Otyepka*[,†]

[†]Regional Centre of Advanced Technologies and Materials, Department of Physical Chemistry, Faculty of Science, Palacky University, 17. listopadu 12, 771 46 Olomouc, Czech Republic

[‡]Department of Pharmacology, Faculty of Medicine and Dentistry, Palacky University, Hněvotínská 3, 775 15 Olomouc, Czech Republic

Supporting Information

ABSTRACT: Cytochrome P450 2C9 (CYP2C9) is a membrane-anchored human microsomal protein involved in the drug metabolism in liver. CYP2C9 consists of an N-terminal transmembrane anchor and a catalytic cytoplasmic domain. While the structure of the catalytic domain is well-known from X-ray experiments, the complete structure and its incorporation into the membrane remains unsolved. We constructed an atomistic model of complete CYP2C9 in a dioleoylphosphatidylcholine membrane and evolved it by molecular dynamics simulations in explicit water on a 100+ ns time-scale. The model agrees well with known experimental data about membrane positioning of cytochromes P450. The entry to the substrate access channel is proposed to be facing the membrane interior while the exit of the product egress channel is situated above the interface pointing toward the water phase. The positions of openings of the substrate access and product egress channels correspond to free energy minima of CYP2C9 substrate ibuprofen and its metabolite in the membrane, respectively.

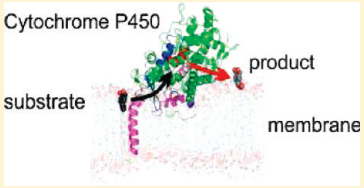

INTRODUCTION

Cytochrome P450 enzymes (CYPs) are prominent family of biotransformation enzymes involved in the metabolism of xenobiotics as well as in pathways involving various endogenous compounds.[1] Metabolism of drugs by microsomal CYPs plays an important role in the pharmacological and toxicological effects of drugs as well as in related drug−drug interactions in humans.[2,3] Consequently, the mechanisms whereby CYPs accommodate various substrates and oxidize them in a stereo- and regio-specific manner are a topic of great interest in the biochemistry of the CYPs. Current insights into determinants of substrate specificity emerging from the available X-ray structures and biochemical data suggest that the mechanism of substrate specificity is complex; involving not only core active site residues but also other structural features, for example, access/egress paths and conformational flexibility.[4−10]

Human microsomal CYPs are anchored in the membrane of the endoplasmic reticulum by their N-terminal sequence.[11,12] However, the structural data available for the CYPs are based on analyses of engineered CYPs without the N-terminal membrane anchor and often with introduced mutations designed to enhance the protein's solubility.[7] As a result, the current X-ray data do not necessarily provide a comprehensive description of the complex structures of the membrane anchored CYPs.[8,9] Despite the growth in the body of data concerning the structural features of CYPs during the past decade, the orientation and position of CYP in the membrane at the atomic level remains unknown. Information about the membrane topology of CYPs is derived from indirect experiments, that is, from epitope search,[12,13] mutagenesis,[14−16] spectroscopy,[17,18] other experimental techniques[18−20] or from models[12,21,22] and calculations based on factors such as the hydrophobicity of amino acid residues.[7,23] These data suggests that other parts of CYP structure, besides the N-terminal membrane anchor, are immersed in the membrane; for example, part of N-terminal domain and the F/G loop.[12,24,25]

One aspect of CYP function involves the oxidation of hydrophobic substrates to make them more hydrophilic (for schematics of the enzyme action see Figure 1). In this respect, a question arises as to how the lipophilic substrates enter the buried active sites of CYPs? From mutation studies, it has been suggested that substrate access channels of CYP enzymes might be located in parts of the protein either in close contact or inside the membrane and that the lipophilic substrates may enter the active site from the membrane via an appropriate access channel.[26] Access channels from family 2 (or pw2, according to Wade's nomenclature[5]) seem to be suitable for passage of substrates to the active site. Similarly another important question is how and where the more hydrophilic products are released from the active site. The solvent channel of CYPs has been identified as a passage enabling active site solvation;[8,27] such a hydrophilic channel may also serve as a potential egress channel for the metabolites.[26] However, the exact positions of the openings of the access/egress channels in respect to the membrane remain to be determined.

Special Issue: Pavel Hobza Festschrift

Received: May 13, 2011
Revised: June 5, 2011
Published: July 11, 2011

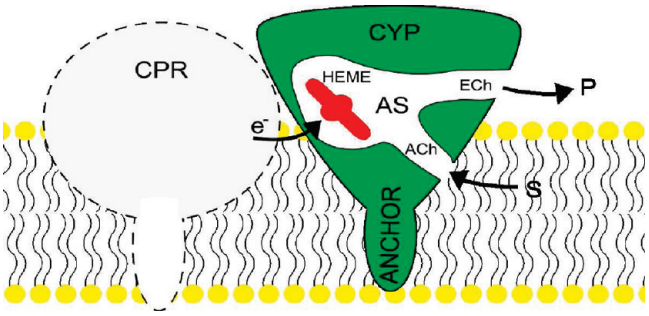

Figure 1. In this work we discuss several structural aspects of CYP2C9 anchored to the membrane at atomic resolution. The scheme shows that it is hypothesized that hydrophobic substrates (S) enter the CYP enzyme active site (AS) via an access channel (ACh). The substrate is oxidized in the active site to a more hydrophilic product (P) and leaves the active site via an egress channel (ECh) to cytosol. The oxidation involves heme (HEME) and requires electrons, which can be provided by cytochrome P450 reductase (CPR).

Here we present an atomic model of the membrane-anchored enzyme CYP2C9, the major CYP2C form in human liver, which is responsible for the biotransformation of both weakly acidic drugs such as ibuprofen and many endogenous compounds.[1,2,28] The model is cross-validated with the available experimental data and provides important information about membrane anchoring, the structural changes CYP2C9 undergoes upon interacting with the membrane and the orientations of the access/egress path within this structure. The calculated free energy profiles of ibuprofen and its metabolite (3-hydroxyibuprofen) show the disposal (penetration depth) of these compounds in the membrane. The mechanisms of substrate access and product release are further discussed with respect to the proposed positions of the substrate and product entrance in/on the membrane.

MATERIALS AND METHODS

Protein Model Building. We used the crystal structure of ligand-free CYP2C9 (PDB ID 1OG2) as a template for model building.[29] The sequence of the engineered CYP2C9 was aligned with the sequence of wild-type human CYP2C9 to detect inserted mutations and with sequences of rabbit CYP2B4 and rat CYP2B1 to compare the experimental data on membrane topology. Multiple alignment was performed using ClustalW2[30] within Jalview 2.6[31] (see Figure S1).

Membrane positioning data were collected mainly from epitope screening of rat CYP2B1 and rabbit CYP2B4,[12,13,32] and from knowledge of phosphorylation[12] and mutations in the CYP2C family.[15,25] Data from epitope screening revealed regions that are inaccessible to the antibodies (i.e., buried inside the protein or within the membrane).

Model building was done in Pymol 0.99rc6.[33] To begin with, the rescue mutations (E206K, V215I, Y216C, P220S, A221P, L222I, L223I) were applied to restore the wild-type sequence of CYP2C9. The transmembrane segment was modeled as α-helix and joined to the rest of the protein by a flexible arm. The protein was then immersed into a membrane modeled on known membrane segments derived from multiple alignment (see Figure S1 in Supporting Information). The transmembrane helix was rotated within the membrane to be approximately perpendicular to the membrane surface.

More than 50% of the membrane of the endoplasmic reticulum consists of phosphatidylcholines.[34] Due to this fact, we based our model membrane on an equilibrated dioleoylpalmitoylphosphatidylcholine (DOPC) membrane with a topology downloaded from http://www.bioinf.uni-sb.de/RB.[35] The membrane was oriented perpendicular to the *z*-axis of the box.

Protein/Membrane Simulation Protocol. Molecular dynamics simulations were used to study the stability of the model with the united-atom GROMOS96 53a6 force field[36] with Berger lipid addition[37] in Gromacs 4.0.7.[38] Parameters of heme were taken from the 53a6 force field. SPC water molecules and chloride and sodium ions were added to neutralize the system and to achieve a cellular salt concentration of 0.1 mM. After energy minimization, 200 ps long prerun was performed to equilibrate water molecules with simultaneous position constraints on protein heavy atoms. The system was then equilibrated in the NPT ensemble for a further 10 ns to equilibrate pressure and box size with an anisotropic Berendsen barostat with a time constant of 10 ps and pressure of 1 bar and V-rescale thermostat with a time constant of 0.1 ps and with temperature of 300 K. Three independent production simulations in the NPT ensemble were then run for a total time of 250 ns. The system equilibrated after 30 ns (for comparison between initial and final model see Figure S2 and for evolution of rmsd see Figure S3 in Supporting Information).

Access Channels Analysis. The access/egress channels were calculated using MOLE (http://mole.chemi.muni.cz) software.[39] MOLE outperforms the previously released CAVER,[40] which is widely used for studies of biomolecular channels and has been successfully applied to the study of CYPs.[5,8,41]

Drug Disposition Simulations. To establish the disposition of drugs in the membrane/water environment, the respective drug molecules were subjected to simulation in the same DOPC/water environment. Gromos96 parameters for the model drug (in this case ibuprofen, a typical substrate of CYP2C9) and its metabolite (3-hydroxyibuprofen) were obtained from the Dundee PRODRG 2.5 Beta server.[42] Ibuprofen (and also 3-hydroxyibuprofen) was modeled in both its uncharged and charged protonation states. Free energy profiles were calculated with the g_wham program.[43] Profiles were calculated by umbrella sampling of the potential of mean force on 45 windows with spacing of 1 Å defined on the membrane normal using a harmonic potential with a force constant of 1000 $kJ \cdot mol^{-1} \cdot nm^{-2}$. Each window was run twice for at least 3 ns: the windows with substantial gradients were run for a longer period with twice as high force constant to minimize error. Starting structures for each window were obtained from free simulations with the molecule starting in water or from pull simulations with force applied on the drug in the direction normal to the membrane.

RESULTS

Model Building. The N-terminal sequence missing from the initial X-ray structure PDB ID 1OG2[29] was modeled as an α-helix. The α-helix topology is typical for a single transmembrane segment as it is able to accommodate the hydrogen bonding of the main-chain atoms in a nonpolar environment. The α-helical topology was consistent with the findings of an NMR study of the N-terminal transmembrane segment from prostaglandin I2 synthase (also known as CYP8A1).[44] The transmembrane α-helix was terminated by a positively charged N-terminus.[1] The α-helix was attached to the CYP2C9 structure

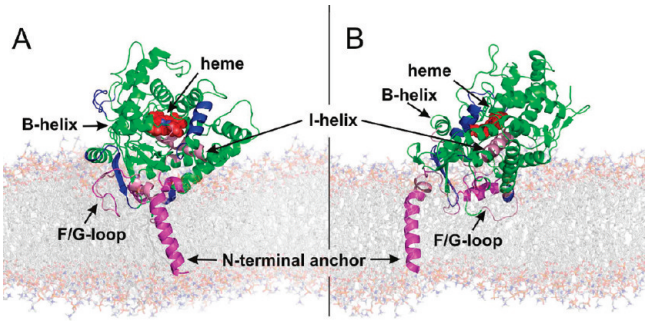

Figure 2. Snapshot of the structure of CYP2C9 in DOPC membrane taken at 50 ns. The protein is shown in green, while parts determined by epitope screening as not being exposed to water (i.e., in the membrane or inside the protein core) are shown in violet. Parts predicted to be accessible to water are shown in blue. Heme is shown by red spheres. The DOPC membrane is shown using the transparent stick representation with orange spheres at the positions of phosphorus atoms in the lipid beads. The image was prepared with Pymol 0.99rc6.[33].

and the mutations introduced into the 1OG2 structure were modified to the native wild-type sequence of CYP2C9. The initial orientation of the CYP2C9 structure on the membrane as well as the depth of the part embedded in the membrane were based on known experimental data from epitope labeling, which indicate parts of CYP inaccessible to the antibodies, that is, those inside the protein or within the membrane.[12,13,32] Arbitrary orientations of the CYP2C9 with respect to the membrane were chosen for molecular dynamics (MD) simulations and all of these systems relaxed to the topology resembling the orientation of the final model (data not shown). A snapshot taken from the equilibrated part of our simulation was used as a final model (Figure 2).

The model presented here provides some new insights and answers, but it should be noted that the model is based on classical MD simulations, which are limited mainly by the quality of the empirical force field and available time scales. The 100 ns long time scale of MD simulation enables limited sampling of the conformational space, that is, the molecules typically fluctuate close to their starting structures (this limitation is also known as the "local conformational trap"). Enhanced sampling can be in principle achieved, for example, by coarse-grained MD simulations using even more simplified coarse-grained potentials. The coarse-grained simulations, however, may suffer from the charge artifacts and also conformational changes of the protein backbone are not adequately described.[45] Both atomic and coarse-grained MD simulations should be always cross-validated with available experimental data and interpreted with care keeping in mind their inherent limitations.

Final Model Cross-Validation. The most important part of the model building is its cross-validation against available experimental data. In our analysis all of the simulations were stable and the protein was relatively rigid. The membrane topology did not change significantly from that used as an input. From this perspective it is not surprising that the information gathered from the epitope screening,[12,13,32] which was used as the main input information during the model construction (see Methods section for details), were also valid for the final model. The regions inaccessible to the antibodies are inside the protein (positions 93−98, B′-helix, and 287−299, I-helix) or within the membrane (positions 1−46, N-terminal anchor, and 207−220, F/G loop).

Protein rotation studies on several CYPs shows that the tilt angle between the heme plane and the membrane plane is variable for different CYPs from approximately 38 to 78°.[46] The tilt angle between the heme and the plane of the membrane was $(35 \pm 5)°$ in our simulations; however, this is still acceptably consistent with the experimental data.

A tryptophan fluorescence scanning study on CYP2C2 suggested that tryptophan residues within the A-helix and the β2-2 sheet (positions 36, 69, and 380) are positioned within the membrane as their fluorescence was quenched by the probes with nitroxide spin labels on fatty acid tails.[47] The authors concluded that the F/G-loop (position 225) is not localized within the membrane. However, the immersion of the F/G-loop in the membrane is based on observations from previous fluorescent studies,[48] mutagenesis,[15,25,29] and trypsinolysis.[49,50] This apparent paradox could possibly be resolved by considering the homodimerization of CYPs from the 2C family. The dimerization interface in crystal structures of truncated CYP2C8 (which is highly homologous to CYP2C9) is formed by the F/G-loop region even with lipids bound.[51] The F/G loop was also identified recently to be at the dimerization interface even in physiological membranes in addition to the N-terminal signaling domain.[52,53] Dimers are mainly formed at higher concentrations; at lower concentrations, CYP2C8 exists primarily as the monomer.[51] Because the concentrations of CYPs in the tryptophan fluorescence scanning study were quite high due to their increased expression in the insect cells,[47] it is possible that the majority of CYPs were dimers under these conditions and that these dimers were likely in contact by the F/G-loop region. The F/G-loop region also forms the dimeric surface with lipids present in the CYP2C8 crystal structure PDB ID 2NNH.[51] On the other hand, older data from trypsinolysis and epitope searching were mainly collected from studies on microsomes with lower concentrations of CYPs, where the CYPs may be present mainly in the form of monomers. Our model represents a monomeric CYP2C9 with an F/G loop and A′-helix inside the membrane. On the other hand, we cannot rule out a possibility that the membrane position of F/G-loop depends on local conditions (e.g., formation of oligomers) or dynamics equilibrium beyond our simulation time scale.

The position of CYPs in the membrane has also been studied by AFM[19,54] and the Langmuir−Blodgett monolayer technique.[20] It was found that the height of the CYP above the membrane is approximately 3.5 ± 0.9 nm and that it occupies an area of 6.8 ± 0.95 nm^2 in the membrane. Therefore, not only the transmembrane helix of the CYP but also a part of the catalytic domain is partially immersed in the membrane. The maximal height of CYP2C9 above the membrane was ~4 nm in our model and the area of the protein in the membrane was slightly more extensive than 8 nm^2. However, some of the lipid molecules were intercalated between the A′-helix and the F/G loop and they contributed to the enlargement of this area. Taken together, this information suggests that our model fits reasonably well with the available experimental data and is valid for further analyses.

Final Model Description. The protein was stable and relatively rigid in all simulations (see the plot of rmsd in Figure S3). The most flexible parts, according to the calculated root-mean-square fluctuations (RMSF, which can be transformed to B-factors as $B_f = 8/3\pi^2$ RMSF^2), were mostly those of the N-terminal transmembrane helix or the loops which were exposed to water. Interestingly, the F/G loop, flexible in some CYPs,[6] was more rigid in CYP2C9 on the membrane. The central part of the

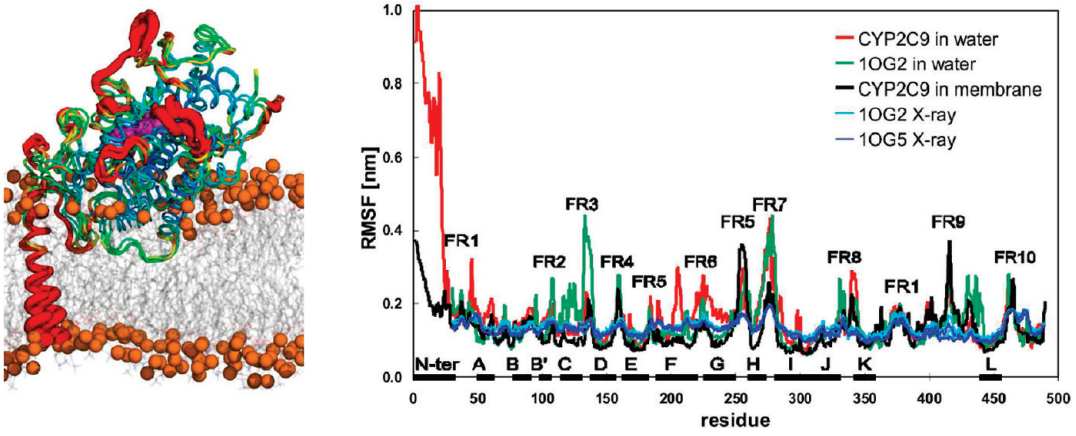

Figure 3. Left panel shows B-factors mapped onto the structure calculated from individual 100 ns long simulations of CYP2C9 in membrane. The B-factors are colored by spectrum from dark blue for rigid regions to red for the most flexible regions. Heme is shown in magenta and membrane lipids are shown in gray with orange spheres for phosphoric atoms. Right panel shows RMSF per residue for simulations of wt CYP2C9 in membrane (black line), wt CYP2C9 in water (green line), CYP2C9 based on crystal structure 1OG2 (without N-terminal anchor) in water (red line), as well as RMSF calculated from the B-factors of crystals structures 1OG2 and 1OG5 (cyan and blue lines, respectively). The figure shows that the most flexible parts of the molecule are the N-terminal anchor (FR1), G/H loop (FR5), K/L loop (FR9), and C-terminus (FR10). Interestingly, the F/G loop, which is flexible in some CYPs, is rather rigid.[6] Also, the central part of the protein close to the catalytic site is relatively rigid. The simulation of CYP2C9 in water shows highly enhanced flexibility of the N-terminal part (FR1) and of the F/G-loop (FR6) in comparison with simulation of CYP2C9 anchored to the membrane. The profiles of RMSF calculated from all simulations have similar trends, which also agree well with published data.[6−8]

protein close to the catalytic site was also rigid (see Figure 3). The flexible N-terminal anchor retained α-helical topology, with a bend at the Arg21 position (see Figure S4 in Supporting Information).

The membrane was rather flexible and it adapted to the presence of the hydrophobic tip of protein composed from the N-terminal transmembrane domain, the A′-helix and the F/G-loop. In the vicinity of the N-terminal anchor, the thickness of the membrane decreased from the initial value of ∼40 Å (the mean distance between two phosphoric groups on the opposite sides of the free DOPC membrane) to ∼33 Å. The adaptation to the protein also resulted in a thickening of the membrane to ∼46 Å in the contact region close to the F/G and K/L loops. After 10 ns of equilibration in the simulation, there were no other significant changes in the membrane topology.

To function, CYPs require CYP reductase (CPR) as a source of electrons (cf. Figure 1). CYP and CPR are both membrane-bound proteins[55] and the membrane facilitates contact between the proteins. The final model should therefore enable CYP/CPR complex formation. The positions of interacting residues were detected experimentally by mutational study on the affinity of CYP2B4 toward CPR.[56] The corresponding residues in CYP2C9 are K121, R125, R132, F134, M136, K138, K432, and G442 (see Figure S1). All of these residues on the surface of the CYP2C9 are accessible to water and available for interaction with CPR in our model (Figure 4).

Effects of the Membrane on the CYP Structure and Flexibility. The RMSF profile calculated from the simulation of CYP2C9 based on 1OG2 X-ray structure agrees well with published results and displays the previously identified common flexible regions.[6,8] The simulation of CYP2C9 with the attached N-terminal anchor displays a similar RMSF pattern besides the extremely flexible N-terminal anchor. The simulation of CYP2C9 in the membrane also shows the same RMSF pattern as simulations of CYP2C9 in water. However, the flexibility of the part of the enzyme in contact with the membrane (specifically the N-terminal part and the C/D and F/G loops) is somewhat decreased. The diffusion of CYP2C9 is also slowed by the presence of the membrane (see Table S1 in Supporting Information).

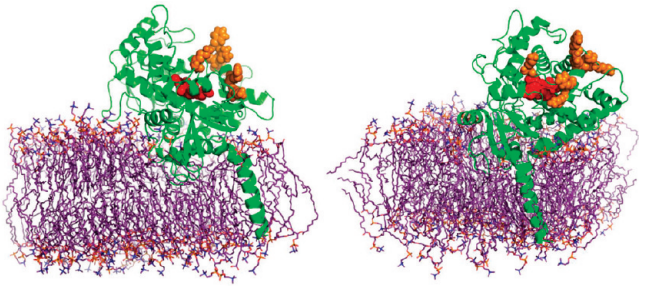

Figure 4. Proximal side of CYP2C9 anchored to DOPC membrane is accessible to water and CYP reductase (CPR). These two views of CYP2C9 show amino acids responsible for binding to CPR (K121, R125, R132, F134, M136, K138, K432, and G442 shown in orange and heme shown in red). These amino acids are present on the CYP proximal side surface.[56] CPR-binding amino acids are accessible to water in our model.

DISCUSSION

Comparison to Empirical Membrane Topology Models from the Literature. Previous studies have attempted to predict CYP membrane topology on the basis of the surface hydrophobicity and available experimental data; our model of wt CYP2C9 is the first atomistic model of the membrane topology. Figure 5 shows a comparison of these predictions and their variabilities. The most similar positioning to our atomistic model provided by the PPM 2.0 computational approach[23] is applied to the complete wt CYP2C9 structure with the N-terminal anchor (cf. white and orange membrane planes in Figure 5). The main difference is in the change in the membrane thickness in the vicinity of the CYP, which is not accounted for in PPM calculations.

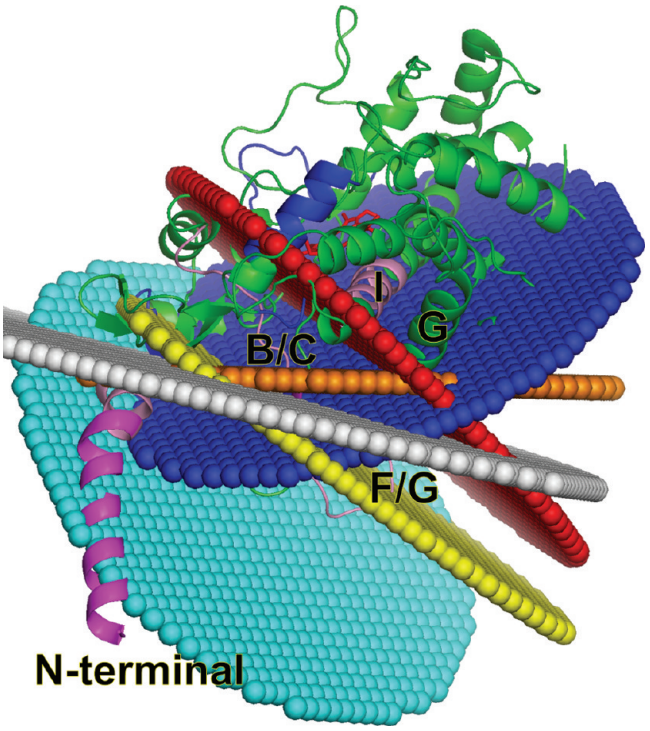

Figure 5. Comparison of models of embedding the CYP2C9 protein into the membrane. Planes of membrane upper layer (approximately at the glycerol level) are colored as follows: This work (orange), Williams et al.[25] (yellow), Wade et al.[57] (cyan), Zhao et al.[59] (red), Lomize et al. PPM 2.0 protein membrane positioning approach for 1OG5 from OPM database http://opm.phar.umich.edu/[23] (blue), and the same PPM 2.0 approach applied to on our wt CYP2C9 model with the N-terminal anchor present (white). As the OPM database shows the planes of positions for the hydrophobic slab, PPM planes were shifted by 10 Å upward to be consistent with other planes at the glycerol level.

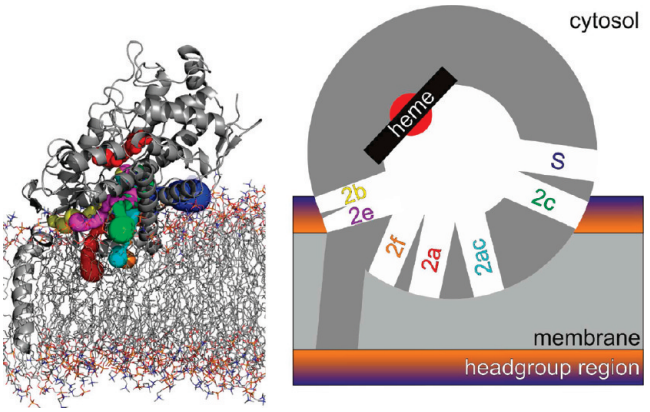

Figure 6. Positions of access/egress channels within membrane anchored CYP2C9. Left panel shows the model of CYP2C9 in DOPC membrane. Protein is shown in dark gray cartoon representation. Heme is shown by red balls. DOPC membrane is shown in wires. The most widely open active site access channel is solvent channel (blue). The mouth opening of the solvent channel is slightly above the membrane-water interface. Channels from 2x family are shown in an order following their opening during the simulation (see Figure S5 in Supporting Information) as follows: 2c (green), 2ac (cyan), 2b (yellow), 2e (magenta), 2f (orange), and 2a (red). All of the openings of these channels are pointing into the membrane; however, the 2b and 2c channel openings are pointing into the headgroup region interface. Access channels were analyzed by MOLE[39] with Pymol 0.99rc6.[33] Right panel shows schematical description of the positions of above-mentioned channels of our model.

If the transmembrane segment is not present (1OG2), the prediction incorrectly exposes residues around the N-terminus to the solvent (Figure 5, blue). The other topologies adopted from the literature indicate that the N-terminus should be inside the membrane, but they show either too shallow immersion of CYP, as shown in Figure 5, in cyan,[57] in yellow,[58] or deeper immersion.[59]

Effects on Access and Egress Channels of CYP2C9. An intriguing question of CYP biochemistry is how substrates enter and products leave the active site, which is buried deep inside the CYP structure. The active site is connected to the outside environment by a network of access/egress channels, which may enable passage of a substrate to, and a product from, the active site.[5,57,60−62] However, there are at least two important and unanswered questions. Does the CYP molecule undergo a large conformational change during substrate binding and product release and which channels enable access and which enable egress?

Our MD simulations do not show any large conformational changes in the CYP2C9 anchored to the membrane. CYP2C9 retains its topology and RMSF indicates decreased fluctuations of CYP2C9 in the membrane in respect to CYP2C9 in water. This implies that common structural features and variations of CYP, derived from X-ray structures of engineered CYPs,[7] are also valid for wild-type CYPs. However, some larger structural changes (namely, in the active site upon binding of larger substrates[63]) of membrane-anchored CYP cannot be ruled out because of the above-mentioned limitation of our MD simulations.

The access/egress channels were analyzed by MOLE software.[39] We adopted the nomenclature of access/egress channels introduced by Wade and co-workers.[5] The X-ray structure of 1OG2 indicates the possible active site access paths, the solvent channel and the 2c channel (between the B′ and G helices). During the MD simulations of CYP2C9 in water the solvent channel closes and the 2c channel opens wider. The analysis of the final model of CYP2C9 in the membrane identified the solvent channel as the widest active site access channel (for further analysis, see Figure S5 in Supporting Information). Solvent channel points slightly above the interface between the membrane and water. Channels from the 2x family (which are mostly closed having bottleneck radii below 1.5 Å) are pointing into the membrane; whereas 2b and 2c channel openings are facing the interface (see Figure 6).

Effects on Drug Disposition and Metabolism. To shed some light to the question how substrates enter and products leave the CYP buried active site, we investigated the position (penetration depth) of a typical CYP2C9 substrate, ibuprofen and its metabolite (3-hydroxyibuprofen), in the membrane. The positions were identified as minima on the free energy profiles along the *z*-axis, which was perpendicular to the membrane (see Figure 7). Potential of mean force simulations on the DOPC membrane/water boundary showed that the free energy profiles of both molecules have different positions of minima (see Table 1). While negatively charged ibuprofen prefers to be inside the membrane perpendicular to the membrane plane with its carboxyl group attached to the positively charged choline group in the DOPC bead, the neutral ibuprofen prefers the hydrophobic membrane interior (see Figure 7). The position of ibuprofen agrees with previous work by Boggara and Krishnamoorti.[64] In contrast, the hydroxylated metabolite is only weakly bound to the

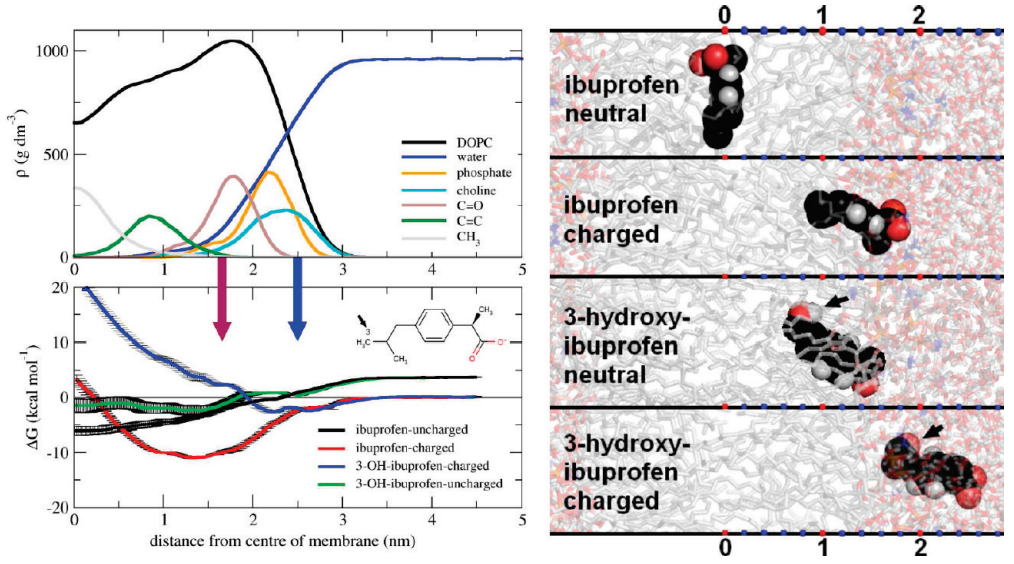

Figure 7. Positions of CYP2C9 substrate ibuprofen and its metabolite on membrane. The upper left part shows partial densities of selected groups on the DOPC membrane/water boundary, while the lower part shows free energy profiles for ibuprofen and 3-hydroxyibuprofen. Free energies were calculated by the potential of mean force imposed on the distance in the *z*-axis between the center-of-mass of the drug and membrane. Zero free energy was arbitrarily selected in the distance of 3.5 nm from the center of the membrane (i.e., in water). The free energy profile for uncharged ibuprofen was shifted by the free energy calculated from the ibuprofen acidity constant in water and for pH 7 by 3.5 kcal/mol (14.6 kJ/mol). The scheme of protonated ibuprofen highlighted with an arrow shows the oxygenation site at position 3 and approximate positions of the opening for 2x and solvent channels are shown by magenta and blues arrows, respectively. The structures on the right side were selected from the window taken from umbrella sampling with minimal free energy. Note that while neutral ibuprofen is in the center of the membrane without any contact with the water environment, both charged molecules are in contact with water molecules mediated by their charged carboxylic group (shown in red). The more polar 3-hydroxyibuprofen is however more exposed to water by its hydroxyl group as shown by black arrow. The figure was prepared in Pymol 0.99rc6.[33].

Table 1. Free Energy Minima for Molecules in DOPC Membrane[a]

	minimum of free energy	
molecule	distance from center of membrane [nm]	ΔG [kcal/mol] (kJ/mol)
ibuprofen (neutral, charge 0)	0.1	−9.6 ± 0.7 (−40.2 ± 2.9)
ibuprofen (charge −1)[b]	1.4	−11.0 ± 0.1 (−46.0 ± 0.4)
3-hydroxyibuprofen (neutral, charge 0)	1.4	−2.4 ± 0.8 (−10.0 ± 3.3)
3-hydroxyibuprofen (charge −1)[b]	2.2	−2.7 ± 0.1 (−11.3 ± 0.4)

[a] Data were calculated by the potential of mean force simulations on DOPC/water membrane. The distance of the carboxylic group to the center-of-mass of the ibuprofen is approximately 5 Å. See Figure 7 for structures corresponding to respective minima. [b] Preferential form in water at pH = 7 (ibuprofen pK_a = 4.44, the same value was also used as a guess for 3-hydroxyibuprofen).[67]

membrane surface and its incorporation into the membrane is energetically highly disadvantageous (see Figure 7). The incorporation of small and rigid molecules (such as cholesterol) is connected with changes in the membrane flexibility and phase transitions.[65] In this respect, it can be hypothesized that CYPs may "sweep out" the membrane by increasing the solubility of low-polar xenobiotics in water, for example, ibuprofen.

It should be noted that there is a significant energy penalty for charged forms for crossing the membrane, whereas uncharged forms prefer the central part of the membrane. The penalty is connected with the introduction of a water-filled hole in the membrane structure, which is filled by the water molecules attached to the charged carboxylic group of ibuprofen. Therefore, a possible model of transfer of ionizable drug across the membrane consists of these steps: (i) the drug is attached into the membrane interior with part of the molecule, (ii) the drug is neutralized, (iii) the drug is transferred across the membrane center, and (iv) the drug is recharged on the other side of membrane. The height of the energy barrier across the membrane and depth of free energy minima define the drug penetration across the membranes and drug partitioning between water and membrane.[66] Both of these properties contribute to determining the drug disposition in the organism.

The minimum of free energy for ibuprofen is located at the position bellow the phosphate groups. This position corresponds approximately to the entrance to the 2x channels. On the other hand, the minimum for 3-hydroxyibuprofen is located approximately at the position of the solvent channel mouth opening (Figure 7). Hence, we can further hypothesize that the 2x channels are involved in the substrate access into the CYP active site and the solvent channel is used for the metabolite egress. This also coincides with information from studies that show that the solvent channel is lined by polar residues enabling active site solvation[8,27] and the 2x channels are in this respect considerably less polar. On the other hand, we cannot rule out the possibility that other (e.g., more polar) substrates can enter the active site via solvent channel and also that some substrates can share the same path for substrate access and product egress.

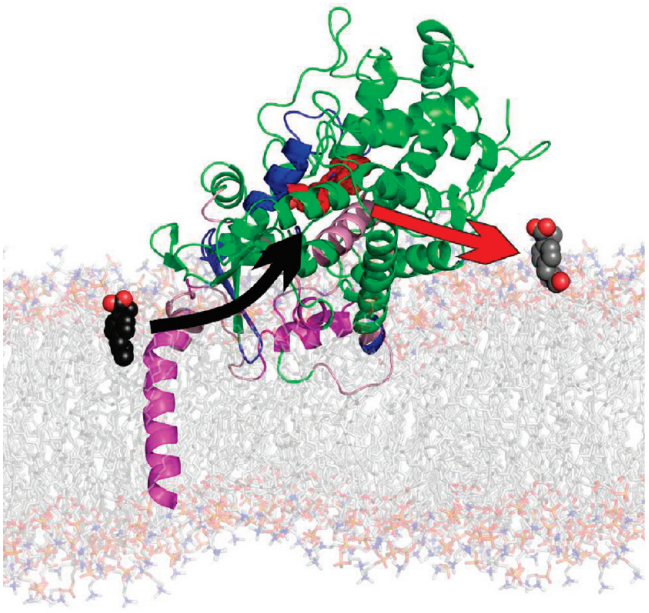

Figure 8. Proposed mechanism of CYP2C9 substrate access and product release. Ibuprofen is accumulated in the membrane, from which it can be effectively "hoovered" by access channels leading to the CYP active site, and following the enzymatic reaction the resulting metabolite may be released via egress channels leading to the cytosol.

CONCLUSIONS

We have constructed an atomic model of CYP2C9 in DOPC membrane; its features were cross-validated with available experimental data from epitope screening, atomic force microscopy measurements, mutagenesis, and fluorescence studies. This model is also consistent with homodimerization and interaction of CYP2C9 with the CYP reductase. The transmembrane helix, 1−1 sheet, A′, G′ helices are located within the membrane, while A, B′, F′, G helices are located on the membrane surface. The membrane anchor is mostly α-helical and is kinked in the membrane at position R21.

The entrance (mouth opening) of the 2x channels points toward the hydrophobic part of the membrane and position of their openings corresponds to the free energy minimum (∼1 nm deep in the membrane) of ibuprofen, which is a CYP2C9 substrate. The mouth opening of solvent channel is positioned in the membrane/solvent interface, corresponding to the minima of free energy profile of the ibuprofen oxidation product on the membrane/water environment (see Figure 8). Therefore, 2x channels (possibly with exception of 2b, 2c, and 2e channels) may be involved in substrate binding (at least of low polar substrates), and the solvent channel is likely to be involved in the product release. The proposed mechanism of drug-binding may be shared among all membrane-bound microsomal CYPs.

ASSOCIATED CONTENT

Supporting Information. Multiple alignment with aggregated information about membrane insertion, table with diffusion coefficient changes, and other figures. This material is available free of charge via the Internet at http://pubs.acs.org.

AUTHOR INFORMATION

Corresponding Author
*E-mail: michal.otyepka@upol.cz.

ACKNOWLEDGMENT

Analysis of channel opening was kindly provided by Vlad Cojocaru from Department of Cell and Developmental Biology, Max Planck Institute for Molecular Biomedicine in Muenster. K. B. would like to thank Kateřina Holá for her help with schematic figures. Support through GACR grants 303/09/1001 and 203/09/H046 and by Student Project PrF_2011_020 of Palacky University are gratefully acknowledged. This work was supported by the Operational Program Research and Development for Innovations - European Social Fund (CZ.1.05/2.1.00/03.0058, CZ.1.05/2.1.00/01.0030 and CZ.1.07/2.3.00/20.0017).

REFERENCES

(1) Ortiz de Montellano, P. R. *Cytochrome P450: Structure, Mechanism, and Biochemistry*, 3rd ed.; Kluwer Academic/Plenum Publishers: New York, 2005.
(2) Anzenbacher, P.; Anzenbacherova, E. *Cell. Mol. Life Sci.* **2001**, *58* (5−6), 737–47.
(3) Coon, M. J. *Annu. Rev. Pharmacol. Toxicol.* **2005**, *45*, 1–25.
(4) Graham, S. E.; Peterson, J. A. *Arch. Biochem. Biophys.* **1999**, *369* (1), 24–9.
(5) Cojocaru, V.; Winn, P. J.; Wade, R. C. *Biochim. Biophys. Acta* **2007**, *1770* (3), 390–401.
(6) Hendrychova, T.; Anzenbacherova, E.; Hudecek, J.; Skopalik, J.; Lange, R.; Hildebrandt, P.; Otyepka, M.; Anzenbacher, P. *Biochim. Biophys. Acta* **2011**, *1814* (1), 58–68.
(7) Otyepka, M.; Skopalik, J.; Anzenbacherova, E.; Anzenbacher, P. *Biochim. Biophys. Acta* **2007**, *1770* (3), 376–389.
(8) Skopalik, J.; Anzenbacher, P.; Otyepka, M. *J. Phys. Chem. B* **2008**, *112* (27), 8165–73.
(9) Pochapsky, T. C.; Kazanis, S.; Dang, M. *Antioxid. Redox Signaling* **2010**, *13* (8), 1273–96.
(10) Fishelovitch, D.; Hazan, C.; Shaik, S.; Wolfson, H. J.; Nussinov, R. *J. Am. Chem. Soc.* **2007**, *129* (6), 1602–11.
(11) Sakaguchi, M.; Mihara, K.; Sato, R. *EMBO J.* **1987**, *6* (8), 2425–31.
(12) Black, S. D. *FASEB J.* **1992**, *6* (2), 680–5.
(13) Black, S. D.; Martin, S. T.; Smith, C. A. *Biochemistry* **1994**, *33* (22), 6945–51.
(14) Szklarz, G. D.; Halpert, J. R. *Life Sci.* **1997**, *61* (26), 2507–20.
(15) Cosme, J.; Johnson, E. F. *J. Biol. Chem.* **2000**, *275* (4), 2545–53.
(16) Nakayama, K.; Puchkaev, A.; Pikuleva, I. A. *J. Biol. Chem.* **2001**, *276* (33), 31459–65.
(17) Fernando, H.; Halpert, J. R.; Davydov, D. R. *Biochemistry* **2006**, *45* (13), 4199–209.
(18) Lepesheva, G. I.; Seliskar, M.; Knutson, C. G.; Stourman, N. V.; Rozman, D.; Waterman, M. R. *Arch. Biochem. Biophys.* **2007**, *464* (2), 221–7.
(19) Bayburt, T. H.; Sligar, S. G. *Proc. Natl. Acad. Sci. U.S.A.* **2002**, *99* (10), 6725–30.
(20) Shank-Retzlaff, M. L.; Raner, G. M.; Coon, M. J.; Sligar, S. G. *Arch. Biochem. Biophys.* **1998**, *359* (1), 82–8.
(21) Hudecek, J.; Anzenbacher, P. *Biochim. Biophys. Acta* **1988**, *955* (3), 361–70.
(22) Friedman, F. K.; Robinson, R. C.; Dai, R. *Front. Biosci.* **2004**, *9*, 2796–806.
(23) Lomize, A. L.; Pogozheva, I. D.; Lomize, M. A.; Mosberg, H. I. *Protein Sci.* **2006**, *15* (6), 1318–33.
(24) Scott, E. E.; He, Y. Q.; Halpert, J. R. *Chem. Res. Toxicol.* **2002**, *15* (11), 1407–13.

(25) Williams, P. A.; Cosme, J.; Sridhar, V.; Johnson, E. F.; McRee, D. E. *Mol. Cell* **2000**, *5* (1), 121–131.
(26) Conner, K. P.; Woods, C. M.; Atkins, W. M. *Arch. Biochem. Biophys.* **2011**, *507* (1), 56–65.
(27) Rydberg, P.; Rod, T. H.; Olsen, L.; Ryde, U. *J. Phys. Chem. B* **2007**, *111* (19), 5445–5457.
(28) Evans, W. E.; Relling, M. V. *Science* **1999**, *286* (5439), 487–91.
(29) Williams, P. A.; Cosme, J.; Ward, A.; Angove, H. C.; Matak Vinkovic, D.; Jhoti, H. *Nature* **2003**, *424* (6947), 464–8.
(30) Larkin, M. A.; Blackshields, G.; Brown, N. P.; Chenna, R.; McGettigan, P. A.; McWilliam, H.; Valentin, F.; Wallace, I. M.; Wilm, A.; Lopez, R.; Thompson, J. D.; Gibson, T. J.; Higgins, D. G. *Bioinformatics* **2007**, *23* (21), 2947–8.
(31) Waterhouse, A. M.; Procter, J. B.; Martin, D. M.; Clamp, M.; Barton, G. J. *Bioinformatics* **2009**, *25* (9), 1189–91.
(32) von Wachenfeldt, C.; Johnson, E. F. Structures of Eukaryotic Cytochrome P450 Enzymes - Membrane Topology. In *Cytochrome P450: Structure, Mechanism and Biochemistry*, 2nd ed.; Plenum Press: New York, 1995; pp 183−223.
(33) DeLano, W. L. *The PyMOL Molecular Graphics System*, 0.99rc6; DeLano Scientific: Palo Alto, CA, 2002.
(34) van Meer, G.; Voelker, D. R.; Feigenson, G. W. *Nat. Rev. Mol. Cell Biol.* **2008**, *9* (2), 112–24.
(35) Siu, S. W.; Vacha, R.; Jungwirth, P.; Bockmann, R. A. *J. Chem. Phys.* **2008**, *128* (12), 125103.
(36) Oostenbrink, C.; Villa, A.; Mark, A. E.; van Gunsteren, W. F. *J. Comput. Chem.* **2004**, *25* (13), 1656–76.
(37) Berger, O.; Edholm, O.; Jahnig, F. *Biophys. J.* **1997**, *72* (5), 2002–13.
(38) Hess, B.; Kutzner, C.; van der Spoel, D.; Lindahl, E. *J. Chem. Theory Comput.* **2008**, *4* (3), 435–447.
(39) Petrek, M.; Kosinova, P.; Koca, J.; Otyepka, M. *Structure* **2007**, *15* (11), 1357–63.
(40) Petrek, M.; Otyepka, M.; Banas, P.; Kosinova, P.; Koca, J.; Damborsky, J. *BMC Bioinf.* **2006**, *7*, 316.
(41) Porubsky, P. R.; Battaile, K. P.; Scott, E. E. *J. Biol. Chem.* **2010**, *285* (29), 22282–90.
(42) Schuttelkopf, A. W.; van Aalten, D. M. *Acta Crystallogr., Sect. D: Biol. Crystallogr.* **2004**, *60* (Pt 8), 1355–63.
(43) Hub, J. S.; de Groot, B. L.; van der Spoel, D. *J. Chem. Theory Comput.* **2010**, *6* (12), 3713–3720.
(44) Ruan, K. H.; So, S. P.; Zheng, W.; Wu, J.; Li, D.; Kung, J. *Biochem. J.* **2002**, *368* (Pt 3), 721–8.
(45) Bond, P. J.; Wee, C. L.; Sansom, M. S. *Biochemistry* **2008**, *47* (43), 11321–31.
(46) Ohta, Y.; Kawato, S.; Tagashira, H.; Takemori, S.; Kominami, S. *Biochemistry* **1992**, *31* (50), 12680–7.
(47) Ozalp, C.; Szczesna-Skorupa, E.; Kemper, B. *Biochemistry* **2006**, *45* (14), 4629–37.
(48) Headlam, M. J.; Wilce, M. C.; Tuckey, R. C. *Biochim. Biophys. Acta* **2003**, *1617* (1−2), 96–108.
(49) Pikuleva, I. A.; Mast, N.; Liao, W. L.; Turko, I. V. *Lipids* **2008**, *43* (12), 1127–32.
(50) Mast, N.; Liao, W. L.; Pikuleva, I. A.; Turko, I. V. *Arch. Biochem. Biophys.* **2009**, *483* (1), 81–9.
(51) Schoch, G. A.; Yano, J. K.; Wester, M. R.; Griffin, K. J.; Stout, C. D.; Johnson, E. F. *J. Biol. Chem.* **2004**, *279* (10), 9497–9503.
(52) Hu, G.; Johnson, E. F.; Kemper, B. *Drug Metab. Dispos.* **2010**, *38* (11), 1976–83.
(53) Szczesna-Skorupa, E.; Mallah, B.; Kemper, B. *J. Biol. Chem.* **2003**, *278* (33), 31269–76.
(54) Nussio, M. R.; Voelcker, N. H.; Miners, J. O.; Lewis, B. C.; Sykes, M. J.; Shapter, J. G. *Chem. Phys. Lipids* **2010**, *163* (2), 182–9.
(55) Kida, Y.; Ohgiya, S.; Mihara, K.; Sakaguchi, M. *Arch. Biochem. Biophys.* **1998**, *351* (2), 175–9.
(56) Bridges, A.; Gruenke, L.; Chang, Y. T.; Vakser, I. A.; Loew, G.; Waskell, L. *J. Biol. Chem.* **1998**, *273* (27), 17036–49.
(57) Wade, R. C.; Motiejunas, D.; Schleinkofer, K.; Sudarko; Winn, P. J.; Banerjee, A.; Kaniakin, A.; Jung, C. *Biochim. Biophys. Acta* **2005**, *1754* (1−2), 239–244.
(58) Williams, P. A.; Cosme, J.; Sridhar, V.; Johnson, E. F.; McRee, D. E. *J. Inorg. Biochem.* **2000**, *81* (3), 183–90.
(59) Zhao, Y.; White, M. A.; Muralidhara, B. K.; Sun, L.; Halpert, J. R.; Stout, C. D. *J. Biol. Chem.* **2006**, *281* (9), 5973–81.
(60) Schleinkofer, K.; , Sudarko; Winn, P. J.; Ludemann, S. K.; Wade, R. C. *EMBO Rep.* **2005**, *6* (6), 584–589.
(61) Li, W. H.; Shen, J.; Liu, G. X.; Tang, Y.; Hoshino, T. *Proteins: Struct., Funct., Bioinf.* **2011**, *79* (1), 271–281.
(62) Fishelovitch, D.; Shaik, S.; Wolfson, H. J.; Nussinov, R. *J. Phys. Chem. B* **2009**, *113* (39), 13018–25.
(63) Ekroos, M.; Sjogren, T. *Proc. Natl. Acad. Sci. U.S.A.* **2006**, *103* (37), 13682–7.
(64) Boggara, M. B.; Krishnamoorti, R. *Biophys. J.* **2010**, *98* (4), 586–95.
(65) McMullen, T. P. W.; Lewis, R. N. A. H.; McElhaney, R. N. *Curr. Opin. Colloid Interface Sci.* **2004**, *8* (6), 459–468.
(66) Orsi, M.; Essex, J. W. *Soft Matter* **2010**, *6* (16), 3797–3808.
(67) Watkinson, R. M.; Herkenne, C.; Guy, R. H.; Hadgraft, J.; Oliveira, G.; Lane, M. E. *Skin Pharmacol. Physiol.* **2009**, *22* (1), 15–21.